Determining the current polarization in Al/Co nanostructured point contacts

F. Pérez-Willard,[1] J. C. Cuevas,[2] C. Sürgers,[1] P. Pfundstein,[3] J. Kopu,[2] M. Eschrig,[2] and H. v. Löhneysen[1,4]

[1]*Physikalisches Institut, Universität Karlsruhe, D-76128 Karlsruhe, Germany*
[2]*Institut für Theoretische Festkörperphysik, Universität Karlsruhe, D-76128 Karlsruhe, Germany*
[3]*Laboratorium für Elektronenmikroskopie, Universität Karlsruhe, D-76128 Karlsruhe, Germany*
[4]*Forschungszentrum Karlsruhe, Institut für Festkörperphysik, D-76021 Karlsruhe, Germany*
(Received 16 January 2004; published 5 April 2004)

We present a study of the Andreev reflections in superconductor/ferromagnet nanostructured point contacts. The experimental data are analyzed in the frame of a model with two spin-dependent transmission coefficients for the majority and minority charge carriers in the ferromagnet. This model consistently describes the whole set of conductance measurements as a function of voltage, temperature, and magnetic field. The ensemble of our results shows that the degree of spin polarization of the current can be unambiguously determined using Andreev physics.

The field of spintronics is largely based on the ability of ferromagnetic materials to conduct spin-polarized currents.[1] Thus, the experimental determination of the degree of current polarization has become a key issue. Recently the analysis of Andreev reflections in superconductor/ferromagnet (S/F) point contacts has been used to extract this spin polarization in a great variety of materials.[2–7] The underlying idea is the sensitivity of the Andreev process to the spin of the carriers, which in a spin-polarized situation is manifested in a reduction of its probability.[8] The theoretical analysis of these S/F point-contact experiments has been mainly carried out following the ideas of the Blonder-Tinkham-Klapwijk (BTK) theory.[9] Different generalizations of this model to spin-polarized systems have been proposed, in which with an additional phenomenological parameter P, the spin polarization of the ferromagnet, excellent fits to the experimental data have been obtained.[2–7] However, a microscopic justification of these models is lacking.[10–12] Recently, Xia *et al.*[13] have combined *ab initio* methods with the scattering formalism to analyze the Andreev reflection in spin-polarized systems. Their main conclusion is that, in spite of the success in fitting the experiments, these modified BTK models do not correctly describe the transport through S/F interfaces. Therefore, at this stage several basic questions arise: what is the minimal model that describes on a microscopic footing the Andreev reflection in spin-polarized systems? More importantly, can the current polarization be experimentally determined using Andreev physics?

In this Rapid Communication we address these questions both experimentally and theoretically. We present measurements of the differential resistance of nanostructured Al/Co point contacts as a function of voltage, temperature, and magnetic field. To analyze the experimental data we have developed a model based on quasiclassical Green functions, the main ingredients of which are two transmission coefficients accounting for the majority- and minority-spin bands in the ferromagnet. We show that this model consistently describes the whole set of data, which unambiguously demonstrates that the spin polarization of current in a ferromagnet can indeed be determined employing Andreev reflection.

We have fabricated Al/Co point contacts following the process described in Ref. 14. Briefly, a bowl-shaped hole is drilled through a 50 nm thick silicon nitride ($Si_{3+x}N_{4-x}$) membrane by means of electron-beam lithography and reactive ion etching. The smallest opening in the insulating membrane has typically a diameter of 5 nm. Finally, 200 nm of Al and $d_{Co}=6$, 12, 24, or 50 nm of Co plus (200 nm$-d_{Co}$) of Cu are deposited by electron-beam evaporation under ultrahigh vacuum conditions ($\sim 10^{-9}$ mbar) on each side of the membrane. A schematic of the samples is shown in Fig. 1(a). The differential resistance R was measured with lock-in technique in a dilution refrigerator. A dc current was superimposed on the small measuring ac component and both R and the voltage drop V were recorded simultaneously.

As a reference we show in Fig. 1(b) the Andreev spectrum, i.e., the differential conductance G as a function of the voltage V of an Al/Cu sample. In all the spectra in this paper, G and V have been normalized by the normal-state conductance G_N and by the zero-temperature superconducting gap Δ of the Al electrode, respectively. G_N showed to be completely independent of V in the range $eV \lesssim (5-10)\Delta$. Since the estimated mean free paths of the Cu and Al electrodes are ~ 60 nm or longer at low temperatures, all the contacts studied are in the ballistic regime. In the Al/Cu case [Fig. 1(b)] the BTK theory fits the experimental data very well (see figure caption for details). In the case of Al/Co, the ferromagnetic layer causes a reduction of the Andreev spectrum amplitude as compared to the Al/Cu contacts (see Fig. 2).
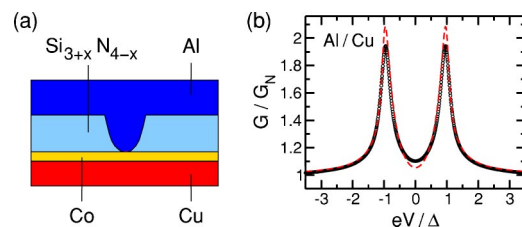

FIG. 1. (Color online) (a) Schematic of an Al/Co nanocontact. (b) Andreev spectrum of an Al/Cu contact at 95 mK (black circles). The dashed line is the fit obtained with the BTK theory (Ref. 9) yielding the transmission $\tau=0.781$ and the gap $\Delta=206$ μeV.
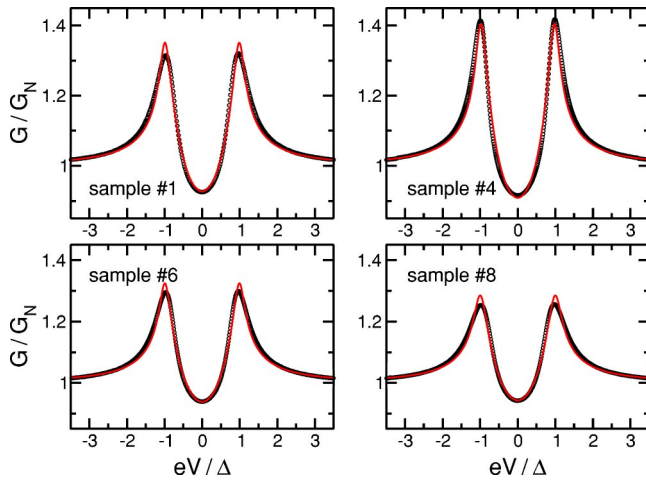
FIG. 2. (Color online) Andreev spectra of four Al/Co point contacts with different Co film thickness d_{Co}. The solid line is a fit to the data with our model (see Table I).

Notice that, although both the normal-state resistances and the Co layer thicknesses of the samples differ strongly (see Table I), the Andreev spectra are all quite similar. This indicates that we are observing an intrinsic property of Al/Co point contacts.

The minimal model necessary to describe transport in S/F contacts should account for the spin-dependent transmission, which is inherent to any junction where ferromagnets are involved. We have developed a model that fulfills this requisite in the framework of the quasiclassical Usadel theory,[15,16] describing a system in terms of two retarded Green functions, $g(\vec{r},\epsilon)$ and $f(\vec{r},\epsilon)$, which depend on both space and energy and satisfy $g^2+f^2=1$. For transport through interfaces this theory must be supplemented with boundary conditions, which can be formulated in terms of a normal-state

scattering matrix $\hat{S}$. Our choice to model a S/F interface is given by (we restrict ourselves to a single conduction channel)

$$\hat{S}=\begin{pmatrix}\hat{r} & \hat{t}\\ \hat{t}^{\dagger} & \hat{r}'\end{pmatrix};\quad \hat{t}=\begin{pmatrix}t_{\uparrow} & 0\\ 0 & t_{\downarrow}\end{pmatrix},\quad \hat{r}=\begin{pmatrix}r_{\uparrow} & 0\\ 0 & r_{\downarrow}\end{pmatrix},\quad (1)$$

where $t_{\uparrow,\downarrow}$ and $r_{\uparrow,\downarrow}$ are the spin-dependent transmission and reflection amplitudes, respectively. The transmission coefficients $\tau_{\uparrow,\downarrow}=|t_{\uparrow,\downarrow}|^2$ are the central quantities of our model. They contain the microscopic properties relevant for transport, i.e., the spin-split band structure of the ferromagnet, the electronic structure of the superconductor, and the interface properties.

The current I_{SF} through the S/F point contact is computed following standard procedures.[17] It can be separated in two spin contributions, $I_{SF}=I_{\uparrow}+I_{\downarrow}$, where each can be written in the BTK form[9]

$$I_{\sigma}=\frac{e}{h}\int_{-\infty}^{\infty}d\epsilon[n_F(\epsilon-eV)-n_F(\epsilon)][1+A_{\sigma}(\epsilon)-B_{\sigma}(\epsilon)],$$
(2)

where n_F is the Fermi function, and $A_{\sigma}(\epsilon)$ and $B_{\sigma}(\epsilon)$ are the spin-dependent Andreev reflection and normal reflection probabilities, respectively. These are given by $A_{\sigma}=\tau_{\sigma}\tau_{-\sigma}|f/\mathcal{D}|^2$ and $B_{\sigma}=|(r_{\sigma}+r_{-\sigma})+(r_{\sigma}-r_{-\sigma})g|^2/|\mathcal{D}|^2$, where $r_{\sigma}=\sqrt{1-\tau_{\sigma}}$ and $\mathcal{D}=(1+r_{\sigma}r_{-\sigma})+(1-r_{\sigma}r_{-\sigma})g$. The Green functions are evaluated right at the interface at the superconducting side. In the point-contact geometry we can ignore the proximity effect, which means that g and f only contain properties of the superconducting electrode. In the case of a BCS superconductor in zero magnetic field $g=-i\epsilon/\sqrt{\Delta^2-\epsilon^2}$ and $f=i(\Delta/\epsilon)g$, and the zero-temperature conductance adopts the form[18]

$$G_{SF}=\frac{4e^2}{h}\begin{cases}\dfrac{\tau_{\uparrow}\tau_{\downarrow}}{(1+r_{\uparrow}r_{\downarrow})^2-4r_{\uparrow}r_{\downarrow}(eV/\Delta)^2}, & eV\leq\Delta\\[3ex] \dfrac{\tau_{\uparrow}\tau_{\downarrow}+(\tau_{\uparrow}+\tau_{\downarrow}-\tau_{\uparrow}\tau_{\downarrow})\sqrt{1-(\Delta/eV)^2}}{[(1-r_{\uparrow}r_{\downarrow})+(1+r_{\uparrow}r_{\downarrow})\sqrt{1-(\Delta/eV)^2}]^2}, & eV\geq\Delta.\end{cases}$$
(3)

In the absence of spin polarization ($\tau_{\uparrow}=\tau_{\downarrow}$) this formula reduces to the BTK result.[9] The normal-state conductance is given by $G_N=(e^2/h)(\tau_{\uparrow}+\tau_{\downarrow})$, and the current polarization is defined by $P=|\tau_{\uparrow}-\tau_{\downarrow}|/(\tau_{\uparrow}+\tau_{\downarrow})$. The main approximation of this model is the assumption that we can describe the point contact with a single pair of transmission coefficients $\tau_{\uparrow,\downarrow}$, which will be finally justified by the agreement with the experiment.

As we show in Fig. 2, using $\tau_{\uparrow,\downarrow}$ and Δ as free parameters our model yields an excellent fit to the Andreev spectra of the Al/Co contacts for temperatures $T\approx100$ mK. These parameters for a total of eight contacts are listed in Table I.

Their deviations from sample to sample are remarkably small, leading to small uncertainties in the mean values given by $\bar{\tau}_{\uparrow}=0.40\pm0.02$, $\bar{\tau}_{\downarrow}=0.98\pm0.01$, and $\bar{\Delta}=(190\pm10)$ μeV. The total current is of course symmetric with respect to the exchange of $\tau_{\uparrow}$ and $\tau_{\downarrow}$, which implies that we cannot assign a transmission coefficient to the majority or minority charge carriers in Co. Nevertheless, we expect the high transmissive coefficient $\tau_{\downarrow}$ to correspond to the minority electrons, because of their higher density of states at the Fermi level corresponding to the Co $3d$ band. In our contacts the mean value of the current polarization is $\bar{P}=0.42\pm0.02$.[19] An analysis of our experimental data for T

TABLE I. Transmissions $\tau_{\uparrow,\downarrow}$, polarization P, and gap Δ for the Al/Co samples as determined by a fit of the Andreev spectra for $T \approx 100$ mK with our model.

Sample	d_{Co} (nm)	R_N (Ω)	T (mK)	Δ (μeV)	$\tau_{\uparrow}$	$\tau_{\downarrow}$	P
1	6	10.4	97	189	0.404	0.979	0.42
2	6	6.69	90	199	0.403	0.979	0.42
3	12	33.2	101	199	0.420	0.968	0.39
4	12	13.3	100	188	0.415	0.970	0.40
5	24	6.00	98	180	0.382	0.989	0.44
6	24	3.58	97	193	0.399	0.983	0.42
7	50	15.7	99	172	0.370	0.994	0.46
8	50	3.59	97	198	0.392	0.986	0.43

≈ 100 mK with the widely used model of Ref. 11 gives fits of similar quality, but yields $\sim 15\%$ smaller values for P. It is important to stress that this model cannot be mapped onto ours, it is not rigorously founded, and misses the fundamental ingredient of a spin-dependent transmission.

The rest of the paper is devoted to illustrate the consistency of the model, and in turn of the determination of the polarization P. We show that fixing the set $\{\tau_{\uparrow}, \tau_{\downarrow}\}$ and Δ, as obtained from the spectra at $T \approx 100$ mK, the model describes without any additional fit parameter the temperature and magnetic-field dependence of the conductance. For instance, in Fig. 3(a) the temperature dependence of the Andreev spectrum of sample No. 2 is depicted. As can be seen, the model describes the whole temperature range by simply using the BCS temperature dependence of the gap. A more stringent test of our model is shown in Fig. 3(b). Here, we compare the temperature dependence of the zero-bias resistance with the theoretical prediction. The agreement is ex-

cellent, apart from the deviations close to the critical temperature. We attribute them to the existence of a stray field (~ 5 mT) created by the Co film. This idea is supported by a calculation (see below for details) of $R(T)$ in the presence of an external field [Fig. 3(b)]. It is worth stressing that $R(T)$ is extremely sensitive to the transmission [see curve for sample no. 3 in Fig. 3(b)], which illustrates the accuracy in the determination of $\{\tau_{\uparrow}, \tau_{\downarrow}\}$.

We have also measured how a magnetic field H parallel to the insulating layer modifies the Andreev spectra [see Fig. 3(c)]. There are three main effects: (i) the height of the two maxima diminishes with increasing field and their positions are shifted to lower voltages; (ii) as can be seen in the inset of Fig. 3(c), the zero-bias conductance is constant for fields below the critical field; (iii) the transition to the normal state is abrupt. To understand these features we now study how the order parameter Δ is modified by the field. We use two approximations: (a) in the Al electrode the mean free path ($l \sim 60$ nm) is much smaller than the superconducting coherence length ($\xi_0 \sim 300$ nm), which justifies the use of the diffusive approximation ($l \ll \xi_0$) and the Usadel theory; (b) for our Al films ξ_0 is greater than the electrode thickness d, which means that we can assume that Δ and the Green functions are constant throughout the sample.

With these approximations the Usadel equation reduces to the generic equation that describes the effect of different pair-breaking mechanisms such as magnetic impurities, supercurrents or magnetic fields:[20]

$$\epsilon + i\Gamma g(\epsilon, H) = i\Delta \frac{g(\epsilon, H)}{f(\epsilon, H)}, \quad (4)$$
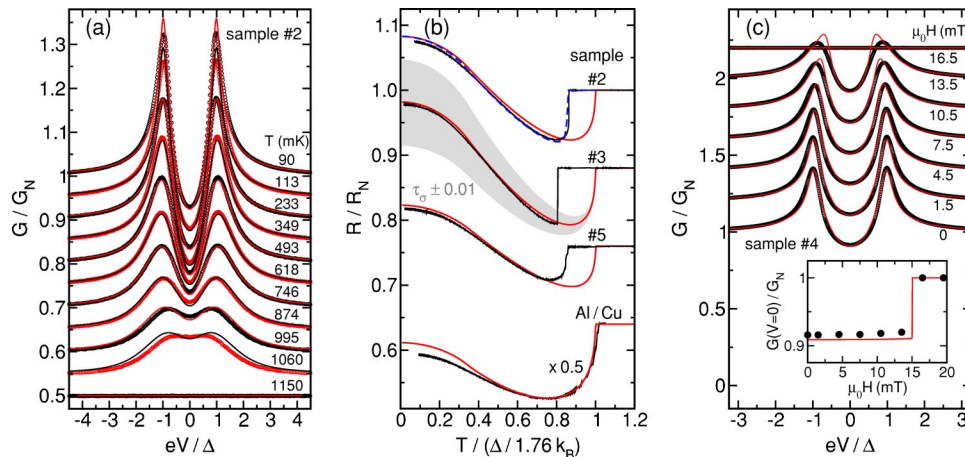
where

FIG. 3. (Color online) (a) Andreev spectrum for sample no. 2 for different temperatures. For clarity, the curves are shifted downwards successively by 0.05 units with increasing temperature. The solid lines are the calculated spectra with our model. (b) Normalized resistance R/R_N as a function of temperature for three Al/Co samples. T is normalized to the gap Δ as obtained from the Andreev spectra (see Table I). The curves are shifted downwards successively by 0.12 units. The red lines are the calculated $R(T)$. For sample no. 2, the dashed line has been calculated including the effect of a residual magnetic field of 5 mT. As a reference, we also show these data for the Al/Cu contact of Fig. 1(b) (the theoretical result corresponds to the nonmagnetic BTK theory). The shaded region is covered by a set of curves given by $\{\tau_{\uparrow} \pm 0.01, \tau_{\downarrow} \pm 0.01\}$ for sample no. 3. (c) Andreev spectrum for sample 4 measured at 100 mK for different magnetic fields. The curves are shifted upwards successively by 0.2 units. The inset shows the zero-bias conductance as a function of the field. The critical field of the sample is $\mu_0 H_c = 15.0$ mT. The red lines are the calculations using $d/\lambda_0 = 3.8$.

$$\Gamma = \frac{2De^2}{\hbar c^2}\langle \vec{A}^2 \rangle,$$

where D is the diffusion constant, Γ is a depairing energy, which contains the effect of the magnetic field, and $\langle \vec{A}^2 \rangle$ is the average value of the square of the vector potential along the thickness of the Al film. Additionally, the order parameter Δ must be determined self-consistently.[16] In Al the London penetration depth is typically $\lambda_0 \sim 50$ nm, which in our case is smaller than the thickness d. This implies that the external field is partially screened inside the sample. Thus, the vector potential appearing in Eq. (4) must be determined solving the Maxwell equation $\nabla^2 \vec{A} = -(4\pi/c)\vec{j}$, where $\vec{j}$ is the supercurrent density given by $\vec{j}(\vec{r}) = -(2\sigma_N/\hbar c)\vec{A}(\vec{r})\int_0^\infty d\epsilon \tanh(\beta\epsilon/2)\mathrm{Im}(f^2)$, where σ_N is the normal conductivity of the Al sample and $\beta = (k_B T)^{-1}$. The solution of the Maxwell equation yields the following expression for the depairing energy:

$$\Gamma(H) = \frac{6\alpha}{r^2\cosh^2(r/2)}\left(\frac{\sinh(r)}{r} - 1\right), \quad \alpha = \frac{De^2d^2H^2}{6\hbar c^2},$$

(5)

where $r = (d/\lambda_0)[(2/\pi)\int_0^\infty d\epsilon' \tanh(\beta'\epsilon'/2)\mathrm{Im}(f^2)]^{1/2}$. Here, the prime indicates that the energy variables are measured in units of the zero-temperature gap in the absence of field, Δ_0, and $\lambda_0 = \sqrt{\hbar c^2/(4\pi^2\sigma_N\Delta_0)}$. In Eq. (5) α is the pair-breaking parameter for a thin film,[20] which can also be written as $\alpha/\Delta_0 = (1/12\pi)[Hd/H_{cb}\lambda_0]^2$, where H_{cb} is the bulk critical field. For Al $\mu_0 H_{cb} = 9.9$ mT. Notice that the ratio d/λ_0 is the only parameter that enters our analysis. Since d/λ_0 de-

termines the critical field of the Al films, H_c, we fix its value by means of an independent measurement of $R(B)$ at $T \approx 100$ mK. For our samples, we find $H_c \approx 1.5 H_{cb}$, which in our theory corresponds to $d \approx 4\lambda_0$. Thus, using Eq. (2) with the self-consistent solution of Eq. (4) for the Green functions, we calculate the magnetic-field evolution of the Andreev spectra, reproducing the main experimental features without any additional parameter [see Fig. 3(c)]. The theoretical analysis of the critical field reveals that for $d > \lambda_0$, as in our case, both Δ and the spectral gap are finite up to the transition to the normal state. This naturally explains why this transition is of first order and why the zero-bias conductance is not modified by the field. The existence of this first-order transition in superconducting films was first discussed in the frame of the Ginzburg-Landau theory.[21]

In conclusion, we have presented a comprehensive experimental study of the transport through Al/Co nanocontacts. We have also introduced a model for the description of the Andreev reflection in S/F interfaces. While retaining the simplicity of BTK-type theories, our model includes the effect of a spin-dependent transmission and allows the analysis of a great variety of realistic ingredients. We have shown that such a model consistently describes the whole set of measurements for arbitrary voltage, temperature, and magnetic field, which demonstrates that the current polarization in ferromagnets can be determined using Andreev physics. Moreover, our data and analysis provide important input for first-principles calculations of electron transmission through ferromagnetic interfaces.

[1] G. Prinz, Phys. Today **48** (4), 58 (1995).

[2] R.J. Soulen, Jr., J.M. Byers, M.S. Osofsky, B. Nadgorny, T. Ambrose, S.F. Cheng, P.R. Broussard, C.T. Tanaka, J. Nowak, J.S. Moodera, A. Barry, and J.M.D. Coey, Science **282**, 85 (1998).

[3] S.K. Upadhyay, A. Palanisami, R.N. Louie, and R.A. Buhrman, Phys. Rev. Lett. **81**, 3247 (1998); S.K. Upadhyay, R.N. Louie, and R.A. Buhrman, Appl. Phys. Lett. **74**, 3881 (1999).

[4] Y. Ji, G.J. Strijkers, F.Y. Yang, C.L. Chien, J.M. Byers, A. Anguelouch, G. Xiao, and A. Gupta, Phys. Rev. Lett. **86**, 5585 (2001).

[5] B. Nadgorny, R.J. Soulen, Jr., M.S. Osofsky, I.I. Mazin, G. Laprade, R.J.M. van de Veerdonk, A.A. Smits, S.F. Cheng, E.F. Skelton, and S.B. Qadri, Phys. Rev. B **61**, R3788 (2000).

[6] P. Raychaudhuri, A.P. Mackenzie, J.W. Reiner, and M.R. Beasley, Phys. Rev. B **67**, 020411(R) (2003).

[7] J.S. Parker, S.M. Watts, P.G. Ivanov, and P. Xiong, Phys. Rev. Lett. **88**, 196601 (2002).

[8] M.J.M. de Jong and C.W.J. Beenakker, Phys. Rev. Lett. **74**, 1657 (1995).

[9] G.E. Blonder, M. Tinkham, and T.M. Klapwijk, Phys. Rev. B **25**, 4515 (1982).

[10] I.I. Mazin, A.A. Golubov, and B. Nadgorny, J. Appl. Phys. **89**, 7576 (2001).

[11] G.J. Strijkers, Y. Ji, F.Y. Yang, C.L. Chien, and J.M. Byers, Phys. Rev. B **63**, 104510 (2001).

[12] Y. Ji, G.J. Strijkers, F.Y. Yang, and C.L. Chien, Phys. Rev. B **64**, 224425 (2001).

[13] K. Xia, P.J. Kelly, G.E.W. Bauer, and I. Turek, Phys. Rev. Lett. **89**, 166603 (2002).

[14] K.S. Ralls, R.A. Buhrman, and R.C. Tiberio, Appl. Phys. Lett. **55**, 2459 (1989).

[15] K.D. Usadel, Phys. Rev. Lett. **25**, 507 (1970).

[16] For a review, see W. Belzig, F.K. Wilhelm, G. Schön, C. Bruder, and A.D. Zaikin, Superlattices Microstruct. **25**, 1251 (1999).

[17] J.C. Cuevas, A. Martín-Rodero, and A. Levy Yeyati, Phys. Rev. B **54**, 7366 (1996); J.C. Cuevas and M. Fogelström, *ibid.* **64**, 104502 (2001); M. Eschrig, J. Kopu, J.C. Cuevas, and G. Schön, Phys. Rev. Lett. **90**, 137003 (2003).

[18] A. Martín-Rodero, A. Levy Yeyati, and J.C. Cuevas, Physica C **353**, 67 (2001).

[19] Notice that P is distinctly different from the spin polarization of the density of states resulting from tunneling experiments. For a review, see R. Meservey and P.M. Tedrow, Phys. Rep. **238**, 173 (1994).

[20] K. Maki, in *Superconductivity*, edited by R.D. Parks (Dekker, New York, 1969), p. 1035. The connection between Eq. (4) and this review is established by $g = -iu/\sqrt{1-u^2}$, where $u\Delta = \epsilon + i\Gamma g$ and $\Gamma = \zeta\Delta$.

[21] P.G. de Gennes, *Superconductivity of Metals and Alloys* (W.A. Benjamin, New York, 1966), p. 189.